

# Evaluation of Aeroelastic Uncertainty Analysis Methods

Brian P. Danowsky,\* Jeffery R. Chrstos,<sup>†</sup> and David H. Klyde<sup>‡</sup>  
*Systems Technology, Inc., Hawthorne, California 90250*

Charbel Farhat<sup>§</sup>  
*CMSoft, Inc., Palo Alto, California 94306*

and  
Marty Brenner<sup>¶</sup>  
*NASA Dryden Flight Research Center, Edwards Air Force Base, California 93560*

DOI: 10.2514/1.47118

**Flutter is a destructive and potentially explosive phenomenon that is the result of the simultaneous interaction of aerodynamic, elastic, and inertial forces. The nature of flutter mandates that flutter flight testing be cautious and conservative. Because of this, further investigation of uncertainty analysis with respect to the flutter problem is desired and warranted. Prediction of flutter in the transonic regime requires computationally expensive high-fidelity simulation models. Because of the computational demands, traditional uncertainty analysis is not often applied to transonic flutter prediction, resulting in reduced confidence in the results. The work described herein is aimed at exploring various methods to reduce the existing computational time limitations of traditional uncertainty analysis. Specifically, the coupling of design of experiment and response surface methods and the application of  $\mu$  analysis are applied to a validated aeroelastic model of the AGARD 445.6 wing. From a high-fidelity nonlinear aeroelastic model, a linear reduced-order model is produced that captures the essential dynamic characteristics. Using reduced-order models, the design of experiment, response surface methods, and  $\mu$ -analysis approaches are compared with traditional Monte Carlo-based stochastic simulation. All of these approaches to uncertainty analysis have advantages and drawbacks. Results from these methods and their robustness are compared and evaluated.**

## I. Introduction

THE potentially explosive nature of flutter mandates that flutter flight testing be cautious and conservative. The development of a flutter stability parameter was undertaken four decades ago to give a more reliable technique to predict the onset of flutter. Other methods of predicting flutter such as damping versus velocity are known to have a number of shortcomings, one of which can be the sudden degradation in damping as illustrated in the explosive flutter example shown in Zimmerman and Weissenburger [1]. In this classic paper, the flutter stability parameter was developed using the classical two-dimensional, two-degree-of-freedom (pitch/plunge) aeroelastic wing model, and the technique was shown to be applicable for higher-degree-of-freedom analysis. The flutter stability parameter (flutter margin) is calculated using the decay rate and damped frequency.

Traditionally, computational aeroelasticity for loads and flutter prediction combines a linear finite element formulation for the structure with linear aerodynamic methods. At the same time, the prediction of aerodynamic performance and control surface effectiveness accounts for the effects of the structural elastic deformations on the external aerodynamics by means of correction factors applied to results obtained when the aircraft is assumed to be rigid. Both practices are well-established in aircraft design and give accurate, reliable, and rather inexpensive predictions for static and dynamic

effects at subsonic and supersonic speeds. In the transonic flight regime and for rapid maneuvering conditions in which nonlinear aerodynamic effects may become nonnegligible, the aircraft design, development, and certification processes rely today on expensive structural and aerodynamic experimental models and on extensive flight testing. Adoption of innovative, unconventional designs and aerodynamically unstable configurations in modern aircraft exacerbates the presence and impact of aerodynamic nonlinearities. A possible consequence of the inaccurate prediction of aerodynamic loads involving nonlinear phenomena; such as shocks, vortices and separated flows; flutter, limit cycle oscillation, and other adverse aeroelastic effects remain unveiled until the flight tests. Unfortunately, flight tests are expensive and can be dangerous. Perhaps for these reasons, a leading aeroelastician at Boeing's Phantom Works wrote in 2001, "The results of a finite number of [nonlinear] CFD [Computational Fluid Dynamics] solutions could be used as a replacement for wind-tunnel testing, assuming a validated code was available" [2], and "Even at present, existing CFD codes should be able to obtain five flutter solutions in 1 yr"[2]. More recently, with the advancement of computational processor speed and memory, state-of-the-art CFD-based nonlinear aeroelastic simulation technologies have become a viable complement to scaled wind-tunnel testing for many types of aeroelastic analyses such as flutter prediction [3,4]. Despite the computational cost savings, high-fidelity models are still relatively expensive and analysis requiring many simulations (i.e., traditional uncertainty analysis) can be extremely burdensome, and in many cases infeasible.

Recently, a team of investigators reported that flight test measurements recorded when different yet similar F-16 aircraft were used for the same set of flutter test missions produced the same trends but exhibited differences in response magnitude [5]. Uncertainties are present in both design-related quantities and operational quantities. The work presented herein will address uncertainty in the first type of quantity; design-related. The behavioral uncertainties relate to the characterization of damage and failures and are best treated by refining the mechanistic models used in describing them. The crucial question remains whether the discrepancies between the numerical results and the experimental data can be eliminated by a more detailed computational model leading to an ever-larger numerical burden or whether the differences are within the bounds of

Presented as Paper 2008-6371 at the AIAA Atmospheric Flight Mechanics Conference and Exhibit, Honolulu, HI, 18–21 August 2008; received 9 September 2009; revision received 9 May 2010; accepted for publication 20 May 2010. Copyright © 2010 by Systems Technology, Inc. Published by the American Institute of Aeronautics and Astronautics, Inc., with permission. Copies of this paper may be made for personal or internal use, on condition that the copier pay the \$10.00 per-copy fee to the Copyright Clearance Center, Inc., 222 Rosewood Drive, Danvers, MA 01923; include the code 0021-8669/10 and \$10.00 in correspondence with the CCC.

\*Senior Research Engineer, 13766 South Hawthorne Boulevard. Senior Member AIAA.

<sup>†</sup>Principal Research Engineer, 13766 South Hawthorne Boulevard.

<sup>‡</sup>Technical Director and Principal Research Engineer, 13766 South Hawthorne Boulevard. Associate Fellow AIAA.

<sup>§</sup>Chief Scientist, 1900 Embarcadero Road. Fellow AIAA.

<sup>¶</sup>Aerospace Research Engineer. Member AIAA.

uncertainties in the structural and fluid models or the scatter in experimental data. The answer to this question will provide key knowledge needed for deciding where to spend future resources for improving prediction capabilities.

Based on previously conducted research using realistic aircraft models, as well as published literature [6,7], the following sources of structural and flow uncertainties have been identified: structural damping, mechanical properties of joints, mass distribution, influence of unmodeled structural components including structural details and flow boundary conditions (i.e., at the engine inlet and outlet), geometry and material properties, roughness of the surface, and flight condition. Clearly, the significance of the uncertainties associated with these parameters depends in great measure on the quantities of interest in the analysis.

The ultimate goal is to significantly reduce the time required to perform aeroelastic uncertainty analysis without sacrificing accuracy. The goal presented herein is to compare uncertainty analysis methods using both design of experiment with response surface methods and robust stability with  $\mu$  analysis. Comparison to a traditional stochastic approach (Monte Carlo analysis) will validate the use of these two methods as much less time prohibitive and computational intensive alternatives that still provide a comprehensive analysis with the same or better level of confidence.

## II. General Overview of Uncertainty Analysis Methods Applied to the Flutter Problem

Traditional flutter prediction uses a deterministic aeroelastic simulation model with parameters representing the as-designed aircraft to calculate the structural damping ratio or flutter margin as a function of airspeed to create the predicted flutter boundary. While not incorrect, outside of the simulation environment, nothing is exactly as designed. Airfoil skin thickness varies, fastener clamping force varies, etc., all of which add uncertainty to the flutter boundary. Thus, flutter margin becomes a confidence interval, rather than an absolute bound.

At its most basic level, the purpose of uncertainty analysis is the estimation of the degree of confidence of the output of a system or model based on known uncertainties in the inputs and system characteristics or model parameters. Input and parameter uncertainties are propagated through a model and the distribution of the model outputs constitute the uncertainty.

Traditional stochastic uncertainty analysis techniques require making multiple, and often many simulation runs. The number of required runs typically scales by a power law based on the number of inputs and parameters with defined uncertainty. Analysis quickly becomes time prohibitive for all but the shortest simulation runs. Therefore goals are to produce efficient, yet still accurate, models and to reduce the number of required simulation runs. This is accomplished with the use of design of experiment with response surface methods and robust stability with  $\mu$  analysis. The widely accepted Monte Carlo approach is used to validate the other more rapid approaches. Overview descriptions of each uncertainty analysis method follow.

### A. Traditional Stochastic Monte Carlo Methods

Monte Carlo methods describe a class of computational algorithms that use repeated random sampling to compute results. These methods primarily involve simulating a physical system repeatedly while randomly changing parameters that the system is dependent on for each simulation. Results are collected and can be analyzed statistically to determine means, standard deviations, maxima, minima and other statistical parameters. With several simulation runs, the results of Monte Carlo approach a continuous surface. The optimal number of runs is that which is a minimum number but produces relatively identical statistical results if more runs are made. By this manner, that minimal amount of runs represents the results as if infinite runs were made. Monte Carlo analysis is used when it is impossible or infeasible to compute exact results with a deterministic approach.

Monte Carlo methods provide a reliable means to analyze problems that are concerned with uncertainty. Uncertain parameters of a physical system are randomly sampled over several runs and the results represent system behavior subject to these uncertainties. Sensitivity to the uncertain parameters is realized by the statistical analysis of the Monte Carlo results. The drawback of these methods is the large amount of runs can be computationally burdensome. If the physical system being modeled is complex and takes a relatively large amount of computational time to run, this burden is amplified by the large amount of simulation runs required to obtain meaningful statistical results.

### B. Design of Experiment and Response Surface Methods

Any system can be described as an input/output relationship. The outputs of a system are dependent on the system inputs and independent parameters. With highly complex or empirical systems that feature large amounts of uncertainty, the input/output relationship of the system in question may be difficult to determine. Response surface methods (RSMs) are used as an accurate approximation to characterize a system's outputs based on variations of the system's inputs and parameters. The design of experiment (DOE)/RSM technique is used to determine an accurate approximate model of a system with minimal sets of input required. The resulting analytical model described by the response surface equation (RSE) is, in most cases, in a simpler form (usually a polynomial) than the original model and is thus more efficient while retaining a level of accuracy.

DOE [8] and RSM [9] are used to significantly reduce the number of full model simulation runs. While Monte Carlo generates random values within the range of input and parameter values, DOE is used to purposely select input and parameter values in order to maximize the information available from the output.

RSEs are used to characterize a system's outputs (referred to as targets) based on variations in its inputs and parameters (referred to as factors). The DOE/RSM technique chooses a RSE that is appropriate for characterizing a particular system, and then designs a set of experiments that will yield maximal information for the regression analysis to fit the RSE to the data. This is the fundamental difference between DOE/RSM and Monte Carlo: Monte Carlo makes no assumption about the relationship between the model output and its inputs/parameters, while DOE/RSM does. The downside for DOE/RSM is that when the form of the RSE is poorly chosen, it yields poor or misleading information. The advantage is that with the properly chosen RSE, the number of full model runs required is cut by an order of magnitude or more.

### C. $\mu$ -Analysis Methods

The  $\mu$  analysis method can be used to determine a mathematically guaranteed robust stability point (flutter boundary) subject to a specified bounded uncertainty. Robust stability and  $\mu$  analysis deal with the stability of the interconnections of stable operators. The small-gain theorem serves as a basis for the determination of stability of the interconnections of stable operators. The small-gain theorem states that a closed-loop feedback system of stable operators (Fig. 1) is internally stable if the loop gain of those operators is stable and bounded by unity [10].

In Fig. 1, the operators  $P$  and  $\Delta$  can be represented by stable transfer function operators. By direct use of the small-gain theorem and properties of the norm, it can be shown that the interconnection is robustly stable if Eq. (1) is satisfied:

$$\|P\|_{\infty} < \|\Delta\|_{\infty}^{-1} \quad (1)$$

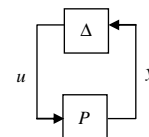


Fig. 1 Closed-loop feedback system of stable operators.

In the above equation,  $\|\cdot\|_\infty$  denotes the infinity norm. Robust stability is analyzed with respect to a set of perturbations. The stability of the interconnection involves a known nominal plant and unknown bounded perturbations (or uncertainties) to that plant. Figure 1 represents a general feedback interconnection of stable operators. Without loss of generality, the known nominal plant dynamics can be represented by  $P$  and the unknown perturbations to that plant can be represented by  $\Delta$ . The true plant is assumed to be a known nominal plant value with perturbations that represent the plant's uncertainty. The small-gain theorem can be used to analyze the stability of the interconnection if the operators are stable and bounded by unity. Although the small-gain theorem guarantees stability of the system, it is overly restrictive, since the structure of the uncertainty is not considered. The  $\Delta$  block, representing the uncertainty in the nominal plant, has a known structure and given this knowledge of the uncertainty structure, a less conservative measure of the robust stability of the system, which is based on the small-gain theorem, can be formulated. This referred to as  $\mu$ , the structured singular value [Eq. (2)]:

$$\mu(P) = \frac{1}{\min_{\Delta \in \Delta} \{\bar{\sigma}(\Delta) : \det(I - P\Delta) = 0\}} \quad (2)$$

In the above equation,  $\bar{\sigma}$  represents the maximum singular value and  $I$  is the identity matrix. Equation (2) is an exact measure of robust stability for any system with a known structured uncertainty, since it only considers uncertainty of the form defined by  $\Delta$ , which represents the bounded space of all possible uncertainty descriptions under the known structure. Given the system in Fig. 1, the plant  $P$  is robustly stable with respect to the set  $\Delta$  if and only if Eq. (3) is satisfied.

$$\mu(P) < \|\Delta\|_\infty^{-1} \quad (3)$$

where  $\mu$  is equivalent to the small-gain theorem [Eq. (1)] if the uncertainty is unstructured. One problem with  $\mu$  is that it is often difficult to compute. Closed-form solutions exist for only a small number of uncertainty structures. Because of this, upper and lower bounds are computed to represent worst- and best-case  $\mu$  values for generalized uncertainty structures.

It is necessary to use the upper bound on  $\mu$  as a basis for analyzing the smallest  $\Delta$  matrix that drives the interconnection unstable, since the upper bound is guaranteed. The lower bound is not guaranteed and may produce a  $\Delta$  matrix that drives the plant unstable. In practice, computing upper and lower  $\mu$  bounds is an optimization problem and is described extensively in public-domain literature [11–13].

### III. Description of the Aeroelastic Reduced-Order Model

#### A. Overview

In this work, the aeroelastic dynamics of the model being analyzed are assumed to take on the form of a linear reduced-order model (ROM). Any aeroelastic system (i.e., fixed cantilever wing or an entire aircraft) can be realized into a linear ROM form. The ROM has many advantages including the ability to determine stability parameters (such as flutter points) without the need for simulation. Simulations can also be conducted using a ROM and are generally much more rapid than simulations that use a full-order high-fidelity model. The ROM is a simplified form of the full-order high-fidelity model that retains essential dynamic characteristics accurately.

A high-fidelity combined CFD and finite element model (FEM) has the capability of simulating very detailed and complex physics with both structural and aerodynamic nonlinearities. A model of high fidelity is required for the transonic flight regime. Linear aerodynamic methods have trouble solving problems in this regime due to the highly nonlinear nature of the flow physics. Traditionally, data is extrapolated from linear models in the subsonic and supersonic regimes to predict the behavior in the transonic regime. Despite the nonlinear nature of the fluid, a model that is linearized

about a point in the transonic regime can be very useful, as it can accurately approximate the dynamic characteristics in a linear operating region. Stability characteristics of a system can be accurately determined from a linear model. A compact linear ROM can be produced directly from a high-fidelity combined CFD/FEM nonlinear aeroelastic model in any flight regime including subsonic, supersonic and transonic [14]. The innovative technique to determine this ROM used herein involves constructing a proper orthogonal decomposition basis from frequency response analysis of the high-fidelity model. Also, the ROMs are based on a fixed Mach number and a fixed orientation and are therefore produced completely nondimensionally. Following the ROM construction process, the fixed nondimensional ROM can be dimensionalized by atmospheric pressure  $p_\infty$  and density  $\rho_\infty$  to produce representations that are valid for any fluid state. Once a linear model is constructed, dynamic characteristics, such as system frequencies, damping and instability (flutter) points can be determined by observing eigenvalues using linear system methods rather than performing full system simulations. Since the flutter problem is, in essence, a linear instability, this ROM serves as an excellent means to analyze this problem.

The linear ROM is essentially a matrix that describes system state behavior [Eq. (4)] and eigenvalue analysis can be used to determine stability characteristics as a function of the fluid state:  $p_\infty$  and  $\rho_\infty$ . If a standard atmosphere model [15] is used, the fluid state is a function of the altitude; therefore, the stability of an aeroelastic ROM can be determined for any altitude  $h$ . ROM flutter points are characterized as neutral stability points and will be a function of  $p_\infty$  and  $\rho_\infty$  or, more simply, a function of  $h$ :

$$\dot{x} = Nx \quad N = f(M_\infty, p_\infty, \rho_\infty) = f(M_\infty, h) \quad (4)$$

In the above equation,  $x$  is the state vector for the linearized aeroelastic system that includes both structural and unsteady aerodynamic states,  $N$  is the matrix representing the ROM, and  $M_\infty$  is the Mach number. A complete analytical representation can be derived for  $N$  as a function of  $p_\infty$  and  $\rho_\infty$  or, using a standard atmosphere model, of  $h$ . This can be accurately approximated as a polynomial in  $h$  [Eq. (5)]. The matrix polynomial coefficients ( $N_0$ ,  $N_1$ , etc.) are based on the fixed Mach number and orientation:

$$N(M_\infty, h) \cong N_0 + N_1 h + N_2 h^2 + \cdots + N_n h^n \quad (5)$$

This polynomial approximation is used for subsequent DOE/RSM and  $\mu$  analysis, which is detailed later herein.

#### B. Aeroelastic ROM in Terms of Structural Parameters and Approximate Relationship

In addition to being a function of the altitude, the ROM is also a function of structural parameters. Assume the structural parameters that vary, or have uncertainty, are collected into the vector  $\beta$ . The ROM nondimensionalized to atmospheric parameters [Eq. (4)] is a function of these parameters as well as the altitude [Eq. (6)]:

$$N = f(M_\infty, h, \beta) \quad (6)$$

Depending on the structural parameters of interest, a complete analytical representation can be derived. Just as was done for the atmospheric parameters, this can be approximated as a polynomial in  $\beta$ . A second-order polynomial is displayed below:

$$N \cong N_0 + N_1 \beta_1 + N_2 \beta_2 + \cdots + N_n \beta_n + N_{1,2} \beta_1 \beta_2 + \cdots + N_{n-1,n} \beta_{n-1} \beta_n + N_{11} \beta_1^2 + \cdots + N_{nn} \beta_n^2 \quad (7)$$

The polynomial in Eq. (7) includes linear terms (e.g.,  $N_0$ ), interaction terms (e.g.,  $N_{1,2}$ ), and squared terms (e.g.,  $N_{11}$ ).

Approximating this polynomial is dependent on the data available for  $N$  as a function of the  $\beta$  parameters. The polynomial approximation (or response surface equation) for  $N$  can be determined by a least squares fit to available data. These data are a series of  $N$  matrices as functions of different  $\beta$  parameter sets. If the size of  $\beta$  is large (i.e., many parameters) it may take many sets of

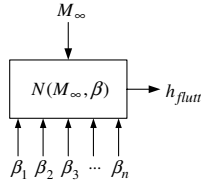


Fig. 2 Model definition.

parameter values to determine an adequate approximation for  $N$ . DOE can be used to determine the parameter sets that will give the best fit for  $N$  while keeping the number of parameter sets to a minimum.

### C. Flutter Point for the ROM and Model Definition

The parameter  $h$  is used to define the stability. The flutter point for a specific ROM is defined as the altitude  $h$  for which one eigenvalue of the ROM matrix  $N$  is directly on the imaginary axis and all other eigenvalues are in the left half of the real complex plane [Eq. (8)]:

$$h_{\text{flutt}} = h \in [h_{\min}, h_{\max}] : \{ \max(\text{Re}(\lambda) : |\lambda I - N(h, M_{\infty}, \beta)| = 0) = 0 \} \quad (8)$$

In the above equation,  $\text{Re}$  represents the operator that extracts the real part of a vector of imaginary numbers. The vectors of imaginary numbers  $\lambda$  are the eigenvalues, which are roots of the system characteristic polynomial. If a polynomial approximation in  $h$  is used for  $N$ , the range of altitudes ( $h_{\min}$ – $h_{\max}$ ) is defined based on the polynomial approximation defined [Eq. (5)]. Following the determination of a flutter altitude, all other parameters that define the flutter point (i.e.,  $V_{\text{flutt}}$ ,  $\omega_{\text{flutt}}$ , etc.) can be found using the Standard Atmosphere, the Mach number and the magnitude of the complex-valued destabilizing eigenvalue.

For all analysis pertaining to uncertainty, this  $h_{\text{flutt}}$  parameter will be used as the dependent parameter for comparison. This parameter, as stated, is a function of the structural parameters.

The model (Fig. 2) is defined as that which produces the flutter altitude for a given set of structural parameters at a specified Mach number. In the case of using the linear aeroelastic ROM, this is determined using Eq. (8). For a more general case, there are many methods that can be used to determine the dependent flutter altitude.

## IV. Uncertainty Analysis Methods Applied to the AGARD 445.6 Wing

The aeroelastic uncertainty analysis methods have been applied to a computational model of the AGARD 445.6 wing (herein referred to as the AGARD wing). This model has been computationally constructed using the coupled CFD/FEM code AERO [4]. This section summarizes the analysis applied to the AGARD wing at two separate Mach numbers. The model is a 2.5 ft, half-span, swept, fixed cantilever wing composed of composite materials. Several configurations of this wing with differing half spans and structural strengths were built and wind-tunnel-tested to their flutter points to compile a comprehensive database of aeroelastic data [16]. Several computational aeroelastic codes have used this data as a benchmark for validation. The versions of the models used for this analysis are the ROMs, which were directly obtained from the full-order, high-fidelity CFD/FEM model.

### A. Aeroelastic ROMs for the AGARD Wing

The AGARD ROMs used for the analysis are a function of several parameters according to Eq. (9).

$$N = f(M_{\infty}, h, \beta_1, \beta_2, \beta_3, \beta_4) \quad (9)$$

This representation includes structural parameter dependence in addition to altitude dependence. The parameters  $\beta_1$  and  $\beta_2$  are two structural parameter multipliers. They represent changes in the structural elastic moduli ( $E_1$ ,  $E_2$ , and  $G_{12}$ ) and structural density,

**Table 1 Nominal flutter altitudes for the AGARD wing**

ROM Mach number	Nominal flutter altitude, ft
0.901	1,257
0.499	−46, 205

respectively. The eigenvalues of the ROM matrix  $N$  exhibit the stability of the aeroelastic system. These eigenvalues are nonlinearly dependent on the atmospheric pressure and density ( $p_{\infty}$ ,  $\rho_{\infty}$ ) and on the structural parameters ( $\beta_1$ ,  $\beta_2$ ). The other parameters,  $\beta_3$  and  $\beta_4$ , represent variations in the local atmospheric pressure and density, respectively. In total, there are four uncertain parameters:  $\beta_1$ ,  $\beta_2$ ,  $\beta_3$ , and  $\beta_4$ . Nominally, the structural parameter multipliers ( $\beta_1$ ,  $\beta_2$ ) and the variation in local atmospheric pressure in density multipliers ( $\beta_3$ ,  $\beta_4$ ) are each equal to one.

The stability at a given set of values for the structural parameters is governed by the altitude. The flutter altitude (i.e., the altitude at which  $N$  is neutrally stable) is a function of the structural parameters  $\beta$  and is governed by Eq. (8). The nominal flutter altitude is found using Eq. (8) and setting  $\beta_1 = \beta_2 = \beta_3 = \beta_4 = 1$ . Table 1 provides these nominal flutter altitudes for the 2 M numbers analyzed.

For the AGARD wing model presented here, the instability is reached with a decrease in altitude. At altitudes below the flutter altitude the system is unstable and contains poles in the right half of the real complex plane. For altitudes above the flutter altitude, the system is stable and contains all left-half plane poles.

### B. Baseline Monte Carlo Analysis for the AGARD ROMs

A baseline Monte Carlo case was run with the four  $\beta$  parameters varying uniformly with a deviation of  $\pm 1\%$  of their nominal value. For this case, 5000 runs were made for both Mach numbers. The resulting output of the Monte Carlo analysis for the Mach 0.901 and the Mach 0.499 ROMs are summarized in histograms in Figs. 3 and 4, respectively. In addition to the histogram data, a normal distribution fit is overlaid with mean and standard deviation  $\sigma$  displayed. In the figures, *value* refers to the flutter altitude and *frequency* refers to the frequency of occurrences at the specified flutter altitude.

The histogram data for the Mach 0.901 case visibly takes the form of a normal distribution. The distribution for the Mach 0.499 case is unusual and does not appear to be exactly normally distributed, especially at the lower altitudes. The important parameter is the least stabilizing altitude, which is the maximum altitude in the distribution (−41, 069 ft). This parameter, representing the least destabilizing robust change in altitude, can be compared with the other analysis methods.

### C. DOE/RSM Analysis for the AGARD ROMs

#### 1. Sensitivity Analysis for the AGARD ROMs: Screening RSE

Generally, for DOE/RSM analysis, a screening RSE is first generated to determine an initial estimate of parameter sensitivity and to determine the goodness of a particular RSE design. Also, screening RSEs are usually generated assuming larger parameter dependence than the final RSE design. A screening RSE was generated for the two AGARD ROMs. Figure 5 displays the nondimensional coefficient relative magnitudes of the quadratic response surface equation fit to the flutter altitude [Eq. (8)]. Also displayed in the figures is a 10% of maximum value line, which clearly distinguishes terms that are an order of magnitude less significant than the greatest term. These fits were determined when the  $\beta$  parameters were allowed to vary by  $\pm 10\%$  of their nominal value for the Mach 0.901 ROM and  $\pm 3\%$  for the Mach 0.499 ROM. A three-level four-factor full factorial design\*\* was selected for each RSE, which required  $3^4 = 81$  runs. The coefficients are based on the quadratic equation (10):

\*\*Quadratic design requires three values ( $1 - \delta$ ,  $1$ ,  $1 + \delta$ ) for each of the four parameters, where  $\delta$  denotes the allowable variation.

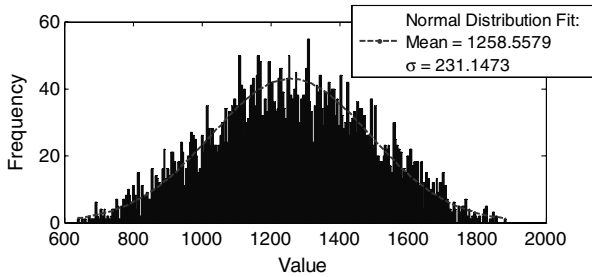


**Fig. 3** Histogram and resulting normal fit to Monte Carlo results for the Mach 0.901 ROM of the AGARD wing.

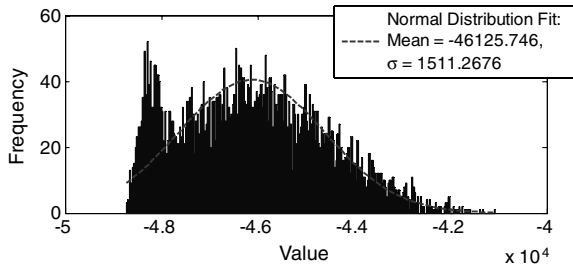
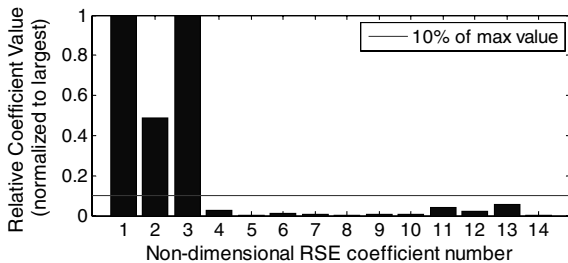


**Fig. 4** Histogram and resulting normal fit to Monte Carlo results for the Mach 0.499 ROM of the AGARD wing.

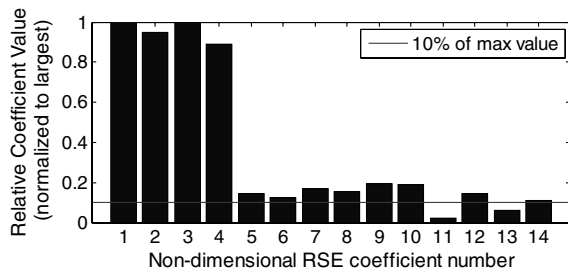
$$h_{\text{flutt}} \cong A_0 + A_1\beta_1 + A_2\beta_2 + A_3\beta_3 + A_4\beta_4 + A_5\beta_1\beta_2 + A_6\beta_1\beta_3 + A_7\beta_1\beta_4 + A_8\beta_2\beta_3 + A_9\beta_2\beta_4 + A_{10}\beta_3\beta_4 + A_{11}\beta_1^2 + A_{12}\beta_2^2 + A_{13}\beta_3^2 + A_{14}\beta_4^2 \quad (10)$$

In the above equations, nondimensional RSE coefficient numbers 1 through 4 are the linear terms, numbers 5 through 10 are the interaction terms, and numbers 11 through 14 are the squared terms.

Observing the results for the Mach 0.901 case (Fig. 5a), it is evident that the flutter altitude is very nearly linearly related to the structural parameter variations in this 10% range, since the first three linear terms are dominant. A linear RSE would most likely suffice in this case. The Mach 0.499 case (Fig. 5b) differs and it is apparent that a quadratic RSE is required, since many of the higher-order terms are greater than 10% of the maximum linear term. Although some



**a) Mach 0.901**



**b) Mach 0.499**

**Fig. 5** Coefficient relative magnitudes of a quadratic response surface equation fitted to the flutter altitude for the AGARD wing ROMs.

parameters were shown to be less significant, all were retained for subsequent analysis, since the design requires a relatively small amount of runs and the final RSE contains a relatively small amount of terms.

## 2. Final RSE Design

A quadratic design for the RSE was selected, since it requires a relatively small amount of experiments (81) and the screening RSE has shown that this quadratic design will be well sufficient. With four parameters, the RSE for the flutter altitude takes on the same form as the screening RSE [Eq. (10)].

A quadratic design with four parameters requires 15 runs (experiments) at a minimum and  $3^4 = 81$  runs at a maximum. A full factorial design with 81 runs was selected, since this number is relatively small. The final RSE was generated assuming only  $\pm 1\%$  variation in the parameters, since this is the assumed level of uncertainty.

According to the screening RSE in Fig. 5, it is evident from the nondimensional RSE magnitudes that the first three linear terms are dominant for the Mach 0.901 ROM. This suggests that a linear RSE including only these terms is most likely adequate. However, maintaining a level of conservatism and considering the fact that a quadratic RSE does not contain many terms, the full quadratic model is retained. Although the interaction and quadratic terms are smaller than the linear terms; keeping the quadratic model will maintain the term's influence at a relatively inexpensive computational cost.

## 3. Monte Carlo Analysis Using the RSE

A Monte Carlo case was run using this quadratic RSE, where a 5000-case simulation was again used with parameters allowed to uniformly vary  $\pm 1\%$  of their nominal value, so that comparisons can be made with the Monte Carlo analysis of the full model.

The results of this analysis is summarized in Fig. 6 for the Mach 0.901 ROM and in Fig. 7 for the Mach 0.499 ROM.

Comparing the results of this analysis (Figs. 6 and 7) with that of the full model (Figs. 3 and 4), it is evident that the RSE accurately approximates the full model in the range of the input parameters (factors) tested. The RSE for the Mach 0.901 ROM produces almost identical results, while the RSE for the Mach 0.499 ROM is not as comparable, but very close. The RSE is a much simpler function and therefore computes much faster than the full model. For this model, the Mach 0.901 RSE Monte Carlo analysis ran 50 times faster than the

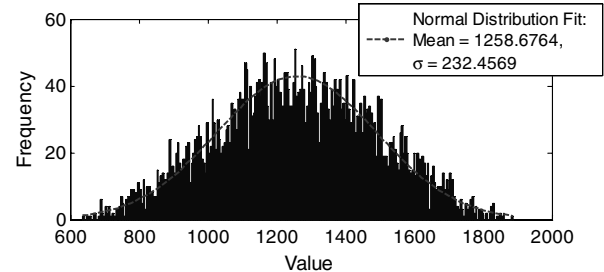


**Fig. 6** Histogram and resulting normal fit to Monte Carlo analysis using the RSE for the Mach 0.901 ROM.

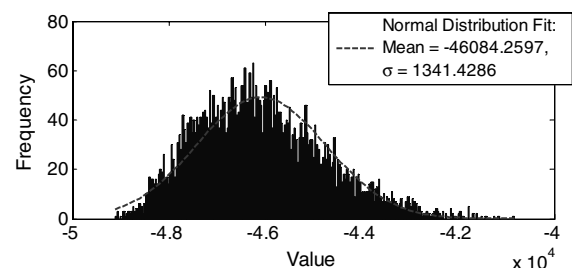


**Fig. 7** Histogram and resulting normal fit to Monte Carlo analysis using the RSE for the Mach 0.499 ROM.

Monte Carlo analysis with the full model. Although the full model did not take long to run itself, this factor of time improvement is impressive and the benefit of an accurate RSE is evident. The time benefits will be realized when more complex aeroelastic models with much longer run times are used.

#### D. $\mu$ -Analysis Approach for the AGARD ROMs

In order for  $\mu$  analysis to be applied, the system (which is represented by a matrix) was first described as a polynomial function of perturbations to the stability parameter  $\delta h$  and perturbations to the uncertain parameters  $\delta\beta$ . To satisfy this polynomial dependence condition, the ROM [N, Eq. (9)] was assumed to be dependent on the altitude by a third-order polynomial and assumed to be linearly dependent on the uncertain parameters  $\beta$  [Eq. (11)]:

$$\begin{aligned} N(\delta h, \delta\beta) = & N_{00} + N_{10}\delta h + N_{20}\delta h^2 + N_{30}\delta h^3 + N_{01}\delta\beta_1 + \dots \\ & + N_{0n}\delta\beta_n + N_{11}\delta h\delta\beta_1 + \dots + N_{1n}\delta h\delta\beta_n + N_{21}\delta h^2\delta\beta_1 + \dots \\ & + N_{2n}\delta h^2\delta\beta_n + N_{31}\delta h^3\delta\beta_1 + \dots + N_{3n}\delta h^3\delta\beta_n \end{aligned} \quad (11)$$

The true dependence on the  $\beta$  parameters is not exactly linear, as shown in the screening RSE (Fig. 5b), but since the higher-order nonlinear terms are much less significant, a linear approximation to the perturbation in  $\beta$  is assumed valid. It is noted that the DOE/RSM technique can be used to generate polynomial fits for the ROM matrix that will benefit the  $\mu$ -analysis technique.

Before applying the uncertainty, a nominal model without uncertainty was constructed, which is dependent on only a variation in altitude [Eq. (12)]:

$$N(\delta h) = N_{00} + N_{10}\delta h + N_{20}\delta h^2 + N_{30}\delta h^3 \quad (12)$$

The flutter altitude can be found with this model that includes no parameter uncertainty and should match that obtained above for each ROM (Table 1). This serves as a useful first check to validate that the methods are being applied correctly.

The  $M$ - $\Delta$  model was formulated from Eq. (12) using a linear fractional transformation approach [11,17–19]. The resulting  $M$ - $\Delta$  feedback configuration in general is displayed in Fig. 8.

A nominal stable altitude is defined as  $h_0$ , and the fixed coefficient matrices in Eq. (12) are dependent on this fixed nominal altitude. A model was constructed in the form of Fig. 8 and an iterative algorithm [11] was used to find the nominal flutter altitudes for each ROM that exactly matched the values in Table 1, validating that the  $M$  matrices are being determined correctly and the third-order polynomial approximation is valid.

The  $M$  structure was then expanded to allow for parameter uncertainty ( $\delta\beta$ ). The coefficient matrices in Eq. (11) were

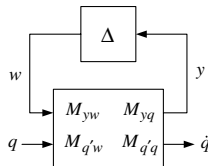


Fig. 8  $M$ - $\Delta$  feedback configuration.

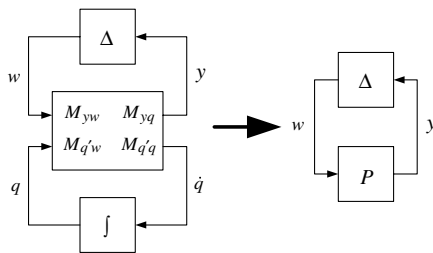


Fig. 9 Formulation of the  $P$ - $\Delta$  model.

Table 2 Robust flutter altitudes determined using the  $\mu$ -analysis method

ROM Mach number	Nominal stable altitude, ft	Nominal flutter frequency, rad/s	Robust flutter altitude, ft	Robust flutter frequency, rad/s
0.901	3,000	112.92	1,980	110.42
0.499	−38,000	599.30	−39,545	596.80

determined using the RSM method. There are 20 coefficient terms in Eq. (11) and that number defines the minimum number of cases to generate a fit. With a maximum power of  $\delta h$  being 3 and the number of  $\beta$  parameters being 4, a full factorial experiment is 64 and this number of experiments was used, since it is relatively small.

To determine  $\mu$ , the bottom loop of the model in Fig. 8 was closed with the integral operator to form the  $P$ - $\Delta$  frequency-dependent model (Fig. 9). The unity norm bound condition was also applied ( $\mu(P) < 1$ ) and due to this, the plant was scaled to account for  $\delta h$  variation greater than unity.

The structured singular value is determined as a function of frequency. An iterative method to determine the robust flutter boundaries was used [11]. A grid of frequency points was selected around the frequency of the nominal flutter velocity. In this initial case the range of frequencies was  $\omega_{\text{flutt}} \pm 5$  rad/s with 5 frequencies evenly spaced. All  $\mu$  computations were performed using the MATLAB®  $\mu$  analysis and synthesis toolbox [20]. The robust flutter altitudes are displayed in Table 2, along with the nominal stable altitudes and the nominal flutter frequencies. Recall that the instability is reached with a decrease in altitude for each Mach number case; therefore, robust flutter altitudes will be greater than the nominal flutter altitude.

By comparing the baseline Monte Carlo results in Figs. 3 and 4 to Table 2, it is apparent that these robust altitudes are in the neighborhood of the maximum flutter altitudes found using the Monte Carlo analysis, providing validation of this estimate. The calculated  $\mu$  bounds vs the frequencies sampled are displayed in Fig. 10 for the Mach 0.901 ROM and in Fig. 11 for the Mach 0.499 ROM. The upper bound was calculated using an implementation from Fan et al. [21], which is detailed by Young et al. [22], and the lower bound was computed using a rapid implementation of the power method [23,24]. Accuracy of the lower bound was not of concern, since only the guaranteed upper bound was needed. The fact

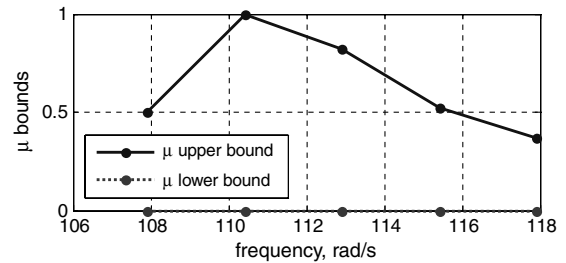


Fig. 10  $\mu(\bar{P})$  vs frequency at the robust flutter altitude for the Mach 0.901 ROM.

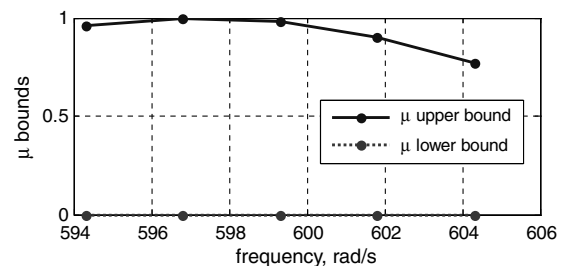


Fig. 11  $\mu(\bar{P})$  vs frequency at the robust flutter altitude for the Mach 0.499 ROM.

**Table 3 Robust flutter altitudes determined from the various methods**

	Nominal flutter altitude, ft	Robust flutter altitudes, ft		
		Monte Carlo	DOE/RSM	$\mu$ analysis
Run time <sup>a</sup>	-46, 205	<i>ROM Mach number 0.499</i>		
		-41, 069	-40, 834	-39, 545
Run time <sup>a</sup>	1257	<i>ROM Mach number 0.901</i>		
		1884	1887	1980
Run time <sup>a</sup>	7 min, 3 s	8 s		
		8 h, 5 min		

<sup>a</sup>On a Dell Precision PWS390, Intel Core2 CPU 6300 at 1.86 GHz. Code is authored and run in MATLAB.

that the upper-bound peaks are within the range of frequencies tested is supporting evidence that the range of frequencies tested is adequate.

### E. Comparison of the Uncertainty Analysis Methods

The robust flutter boundaries vs Mach number determined from all of the methods are collectively displayed in Table 3 and Fig. 12.

It is apparent that all three methods are producing robust flutter altitudes in the same neighborhood of values. This is supporting evidence that each independent method is producing accurate results. The Monte Carlo analysis method, which is the less elegant but thorough and reliably tested approach, is defined as the baseline to compare the other methods against. By this criterion, it is evident that the other two methods; DOE/RSM and  $\mu$  analysis, are producing accurate and representative results. In fact, the other two methods are producing slightly more conservative flutter boundaries with the  $\mu$ -analysis method producing the most conservative robust flutter altitudes. This supports the fact that  $\mu$  is determined over the entire space of all possible uncertainty values that conform to the defined structure and is guaranteed. Essentially,  $\mu$  should produce results that are representative of a Monte Carlo analysis with infinite runs. By this definition, the robust flutter boundaries determined using  $\mu$  should always be either equal to or more conservative than the Monte Carlo analysis, which is suggested by the results herein. Of course, in order to use the  $\mu$ -analysis approach applied herein, a linear system (or approximate) must be used with polynomial dependency on the uncertain parameters. These approximations could lead to inaccurate results if the polynomial approximation is insufficient. The fact that the above results produced robust flutter boundaries that are more conservative than the Monte Carlo analysis approach strongly supports the claim that the approximation is valid and accurately represents the full system.

It is important to address the large computational time burden associated with the  $\mu$ -analysis approach. In this work, the aeroelastic system was assumed to be dependent on the stability parameter that defines the flutter boundary (the altitude  $h$ ) by a third-order polynomial [Eq. (11)]. This causes the corresponding  $\Delta$  structure to be very large and consequently increases the computational burden

associated with the upper-bound  $\mu$  computations. Also, the uncertainty descriptions in this work are purely real, which has proven to cause difficulty in computing  $\mu$  bounds [25]. Introduction of some complex bounded uncertainty would most likely result in more efficient  $\mu$  computations. Alternative approaches for determining robust flutter boundaries with  $\mu$  have been developed recently that do not require the stability parameter to be part of the  $\Delta$  structure or be restricted to polynomial dependency [26–29]. Some recent methods have also introduced complex aerodynamic uncertainty [26], which is undoubtedly present in real-world aeroelastic systems. Efficient computation of robust flutter boundaries, using these approaches, has been demonstrated on an F-16 sample test case by Borglund and Ringertz [30]. Extending the  $\mu$ -analysis approach here to take advantage of aspects from these recent approaches would most likely decrease the computational burden associated with  $\mu$  upper-bound determination.

It is also noted that the structured singular value framework can be exploited to take flight data into account; recent methods have been developed that use measured frequencies and damping values of aeroelastic modes to validate the model at subcritical nonflutter conditions [28]. This capability is extremely attractive for aeroservoelastic clearance of operational aircraft.

## V. Conclusions

The three uncertainty methods (Monte Carlo, DOE/RSM, and  $\mu$  analysis) have been effectively demonstrated for use with an aeroelastic wing model. The model type used for this work is a linear reduced-order model (ROM). This type of aeroelastic model has several advantages; one of which being that flutter solutions are found relatively rapidly without the need for full system simulation.

The validity of the DOE/RSM method has been effectively demonstrated, as the results are almost identical to the baseline Monte Carlo analysis. The computational time advantage of the DOE/RSM method has also been successfully illustrated by the run time improvement, which is due to the fact that the number of runs of the full model has been reduced by two orders of magnitude. This advantage will be more realized as model order and complexity increases.

The  $\mu$ -analysis method has also been shown to produce valid and convincing results. Robust flutter boundaries found using the structured singular value have been shown to compare with the Monte Carlo results very well. The results obtained using  $\mu$  are more conservative and are guaranteed mathematically. Although the increased run time for  $\mu$  analysis is detrimental for the case used here, the mathematical guarantee is extremely valuable. It is important to note that the  $\mu$ -analysis run time is a direct function of the system size, the amount of uncertain parameters and the order of the polynomial dependence of the parameters. Model order reduction and alternative uncertainty descriptions can improve  $\mu$ -computation times: in some cases, significantly.

The  $\mu$ -analysis method demonstrated herein is applicable only if the system is dependent on the uncertain parameters in a polynomial form. The DOE/RSM method can be used to effectively determine approximate system models that are dependent on parameters in a polynomial form. Because of these similarities, the DOE/RSM method has been shown to complement the  $\mu$ -analysis method very well. The work displayed herein has effectively used the DOE/RSM approach to aid  $\mu$  analysis.

Two less traditional aeroelastic uncertainty analysis methods with varying degrees of robustness have been established and tested using an accurate model of the AGARD 445.6 wing, a traditional benchmark model with extensive experimental data. The two methods have shown results that compare very well to the established and widely accepted traditional stochastic Monte Carlo approach.

## Acknowledgments

The work described herein was conducted as part of a Phase I Small Business Innovation Research program sponsored by NASA Langley Research Center in conjunction with NASA Dryden Flight

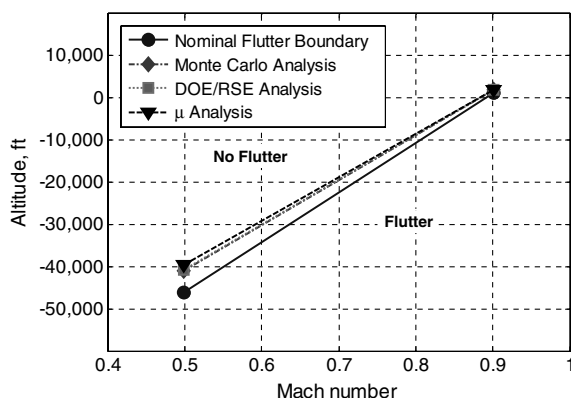


**Fig. 12 Robust flutter boundaries determined from the various methods.**

Research Center. The authors acknowledge NASA for valuable resources and funding.

## References

- [1] Zimmerman, N., and Weissenburger, J., "Prediction of Flutter Onset Speed Based on Flight Testing at Subcritical Speeds," *Journal of Aircraft*, Vol. 1, No. 4, 1964, pp. 190–202.  
doi:10.2514/3.43581
- [2] Yurkovich, R. N., Liu, D. D., and Chen, P. C., "The State-of-the-Art of Unsteady Aerodynamics for High Performance Aircraft," AIAA Paper 2001-0428, Jan. 2001.
- [3] Geuzaine, P., Brown, G., Harris, C., and Farhat, C., "Aeroelastic Dynamic Analysis of a Full F-16 Configuration for Various Flight Conditions," *AIAA Journal*, Vol. 41, No. 3, 2003, pp. 363–371.  
doi:10.2514/2.1975
- [4] Farhat, C., Geuzaine, P., and Brown, G., "Application of a Three-Field Nonlinear Fluid-Structure Formulation to the Prediction of the Aeroelastic Parameters of an F-16 Fighter," *Computers and Fluids*, Vol. 32, Issue 1, 2003, pp. 3–29.  
doi:10.1016/S0045-7930(01)00104-9
- [5] Sussingham, C., DeJoannis, J., and Sansone, A., "F-16 Aeroelastic Flight Testing: Impact on the Operational Fleet," *2000 Report to the Aerospace Profession; Proceedings of the 44th SEPT Symposium*, Los Angeles, Sept. 2000, pp. 122–141.
- [6] Kuttenukeuler, J., "A Finite Element Based Modal Method for Determination of Plate Stiffnesses Considering Uncertainties," *Journal of Composite Materials*, Vol. 33, No. 8, 1999, pp. 695–711.  
doi:10.1177/002199839903300803
- [7] Kuttenukeuler, J., and Ringertz, U., "Aeroelastic Tailoring Considering Uncertainties in Material Properties," *Structural and Multidisciplinary Optimization*, Vol. 15, Nos. 3–4, 1998, pp. 157–162.  
doi:10.1007/BF01203526
- [8] Montgomery, D. C., *Design and Analysis of Experiments*, 5th ed., Wiley, New York, 2001.
- [9] Myers, R. H., and Montgomery, D. C., *Response Surface Methodology: Process and Product Optimization Using Designed Experiments*, 2nd ed., Wiley, New York, 2002.
- [10] Lind, R., and Brenner, M. J., "Robust Flutter Margin Analysis That Incorporates Flight Data," NASA TP-1998-206543, March 1998.
- [11] Lind, R., and Brenner, M., *Robust Aeroelastic Stability Analysis*, Springer-Verlag, London, 1999.
- [12] Zhou, K., Doyle, J. C., and Glover, K., *Robust and Optimal Control*, Prentice-Hall, Upper Saddle River, NJ, 1996.
- [13] Zhou, K., and Doyle, J. C., *Essentials of Robust Control*, Prentice-Hall, Upper Saddle River, NJ, 1998.
- [14] Lieu, T., Farhat, C., and Lesoinne, M., "Reduced-Order Fluid/Structure Modeling of a Complete Aircraft Configuration," *Computer Methods in Applied Mechanics and Engineering*, Vol. 195, No. 41–43, 2006, pp. 5730–5742.  
doi:10.1016/j.cma.2005.08.026
- [15] "U.S. Standard Atmosphere, 1976," National Technical Information Service, U.S. Department of Commerce, Oct. 1976.
- [16] Yates, E. C., Jr., "AGARD Standard Aeroelastic Configurations for Dynamic Response. Candidate Configuration I-Wing 445.6," NASA TM-100492, Aug. 1987.
- [17] Danowsky, B. P., Chavez, F. R., and Brenner, M., "Formulation of an Aircraft Structural Uncertainty Model for Robust Flutter Predictions," AIAA Paper 2004-1853, April 2004.
- [18] Boukarim, G. E., and Chow, J. H., "Modeling Nonlinear System Uncertainties using a Linear Fractional Transformation Approach," *Proceedings of the American Control Conference*, Inst. of Electrical and Electronics Engineers, Piscataway, NJ, June 1998, pp. 2973–2979.
- [19] Lind, R., "Match-Point Solutions for Robust Flutter Analysis," *Journal of Aircraft*, Vol. 39, No. 1, 2002, pp. 91–99.  
doi:10.2514/2.2900
- [20] Balas, G. J., Doyle, J. C., Glover, K., Packard, A., and Smith, R.,  *$\mu$ -Analysis and Synthesis Toolbox User's Guide*, The MathWorks, Inc., Natick, MA, 1996.
- [21] Fan, M., Tits, A., and Doyle, J., "Robustness in the Presence of Mixed Parametric Uncertainty and Unmodeled Dynamics," *IEEE Transactions on Automatic Control*, Vol. 36, 1991, pp. 25–38.  
doi:10.1109/9.62265
- [22] Young, P., Newlin, M., and Doyle, J., "Practical Computation of the Mixed Problem," *Proceedings of the American Control Conference*, Inst. of Electrical and Electronics Engineers, Piscataway, NJ, 1992, pp. 2190–2194.
- [23] Young, P., and Doyle, J., "Computation of  $\mu$  with Real and Complex Uncertainties," *Proceedings of the 29th IEEE Conference on Decision and Control*, Inst. of Electrical and Electronics Engineers, Piscataway, NJ, Dec. 1990, pp. 1230–1235.
- [24] Packard, A. K., Fan, M., and Doyle, J., "A Power Method for the Structured Singular Value," *Proceedings of 27th IEEE Conference on Decision and Control*, Inst. of Electrical and Electronics Engineers, Piscataway, NJ, Dec. 1988, pp. 2132–2137.
- [25] Hayes, M. J., Bates, D. G., and Postlethwaite, I., "New Tools for Computing Tight Bounds on the Real Structured Singular Value," *Journal of Guidance, Control, and Dynamics*, Vol. 24, No. 6, 2001, pp. 1204–1213.  
doi:10.2514/2.4836
- [26] Borglund, D., "The  $\mu$ -k Method for Robust Flutter Solutions," *Journal of Aircraft*, Vol. 41, No. 5, 2004, pp. 1209–1216.  
doi:10.2514/1.3062
- [27] Borglund, D., "Upper-Bound Flutter Speed Estimation Using the  $\mu$ -k Method," *Journal of Aircraft*, Vol. 42, No. 2, 2005, pp. 555–557.  
doi:10.2514/1.7586
- [28] Borglund, D., "Robust Eigenvalue Analysis Using the Structured Singular Value: The  $\mu$ -p Flutter Method," *AIAA Journal*, Vol. 46, No. 11, 2008, pp. 2806–2813.  
doi:10.2514/1.35859
- [29] Borglund, D., and Ringertz, U., "Solution of the Uncertain Flutter Eigenvalue Problem Using  $\mu$ -p Analysis," *International Forum on Aeroelasticity and Structural Dynamics*, Paper IFASD-2009-048, Seattle, WA, 2009.
- [30] Borglund, D., and Ringertz, U., "Efficient Computation of Robust Flutter Boundaries Using the  $\mu$ -k Method," *Journal of Aircraft*, Vol. 43, No. 6, 2006, pp. 1763–1769.  
doi:10.2514/1.20190